Cubé Resin Insecticide: Identification and Biological Activity of 29 Rotenoid Constituents

Nianbai Fang† and John E. Casida*

Environmental Chemistry and Toxicology Laboratory, Department of Environmental Science, Policy and Management, University of California, Berkeley, California 94720-3112

Cubé resin, the root extract from *Lonchocarpus utilis* and *urucu,* is an important insecticide, acaricide, and piscicide. The four major active ingredients are rotenone, deguelin, rotenolone, and tephrosin, totaling 77 wt %. As a commercial pesticide, the minor constituents are also of chemical interest and toxicological relevance. This study identifies 25 minor rotenoids in cubé resin "brittle" of which 12 are new compounds, the most unusual being 7′-chloro-5′-hydroxy-4′,5′-dihydrodeguelin (the first chlororotenoid from a plant extract) and four isomers of 4′,5′-dihydro-4′,5′-dihydroxytephrosin. Several of the minor rotenoids may be decomposition products from free radical processes during sample preparation, extraction with trichloroethylene, and processing the resin. Assays of the 29 rotenoids as inhibitors of NADH:ubiquinone oxidoreductase activity (primary target for toxicity) and phorbol ester-induced ornithine decarboxylase activity (indicator of cancer chemopreventive action) and for cytotoxicity establish similar structure−activity relationships in each system and the importance of the overall molecular conformation and the E-ring substituents.

Keywords: *Cubé resin; cytotoxicity; insecticide; NADH:ubiquinone oxidoreductase; ornithine decarboxylase; piscicide; rotenoid; rotenone*

INTRODUCTION

Rotenone is the principal active ingredient of cubé resin used as an insecticide, acaricide, and piscicide (Negherbon, 1959; Tomlin, 1997). It is applied to field crops, gardens, and farm animals, resulting in human exposure during application and as residues in food and water. In 1997 rotenone was used to treat Lake Davis in California to achieve the balance of fish species considered to be most desirable by sport fishermen (California Department of Fish and Game, 1997). A recent analysis of the composition of cubé resin extracted from the roots of *Lonchocarpus utilis* and *urucu* from Peru established as the four major ingredients rotenone (44.0%) (**1**), deguelin (22.0%) (**8**), 12aβ-hydroxyrotenone (rotenolone) (6.7%) (**2**), and 12aβ-hydroxydeguelin (tephrosin) (4.3%) (**9**) (Figure 1) (Fang and Casida, 1998) as expected (Crombie, 1963; Fukami and Nakajima, 1971). The minor constituents of pesticides are also of chemical interest and toxicological relevance, and with commercial synthetic products they must be identified and evaluated as to potential toxic properties. The same standard is applied here to cubé resin.

This study isolates and identifies 25 minor rotenoids in cubé resin (Figure 2). Thirteen of them are known compounds from extracts of the same or other **1**-containing Leguminosae, that is, **3**−**7**, **10**, **13**−**16**, **22**, **27**, and **28**. Twelve others are new compounds, that is, **11**, **12**, **17**−**21**, **23**−**26**, and **29**. The 29 rotenoids include 11 variations in the E ring and several in the B and D rings, thereby providing a new and unique set of compounds to elucidate structure−activity relationships in three types of biological systems. The primary target for toxicity is NADH:ubiquinone oxidoreductase, and **1** is the classical inhibitor at this site [reviewed by Hollingworth and Ahammadsahib (1995) and Wood et al. (1996)]. Rotenoids **1** and **2** are also potent inhibitors of phorbol ester-induced ornithine decarboxylase (ODC) activity, which is considered to be an indicator for antiproliferative effect and candidate cancer chemopreventive action (Gerhäuser et al., 1995, 1996, 1997; Rowlands and Casida, 1997, 1998). In addition, compounds **1** and **2** at low micromolar levels are cytotoxic in mouse liver cancer cells (Hepa 1c1c7) and human epithelial breast cancer cells (MCF-7) possibly due to NADH:ubiquinone oxidoreductase inhibition (Fang et al., 1997). The structure−activity relationships of the 29 rotenoids were determined in these three systems to further evaluate the hypothesis (Gerhäuser et al., 1995, 1996, 1997; Fang and Casida, 1998) that inhibition of NADH:ubiquinone oxidoreductase activity is the initial step in both inhibition of induced ODC activity and cytotoxicity.

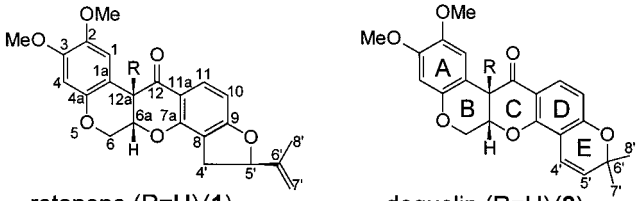

Figure 1. Four principal constituents of cubé resin insecticide showing the general numbering system applied to the various rotenoids.

* Author to whom correspondence should be addressed [telephone (510) 642-5424; fax (510) 642-6497; e-mail ectl@nature.berkeley.edu].

† Present address: Crop Protection Research and Development Group, Uniroyal Chemical Co., Inc., Middleport, CT 06749.

10.1021/jf981188x CCC: $18.00
Published on Web 04/21/1999

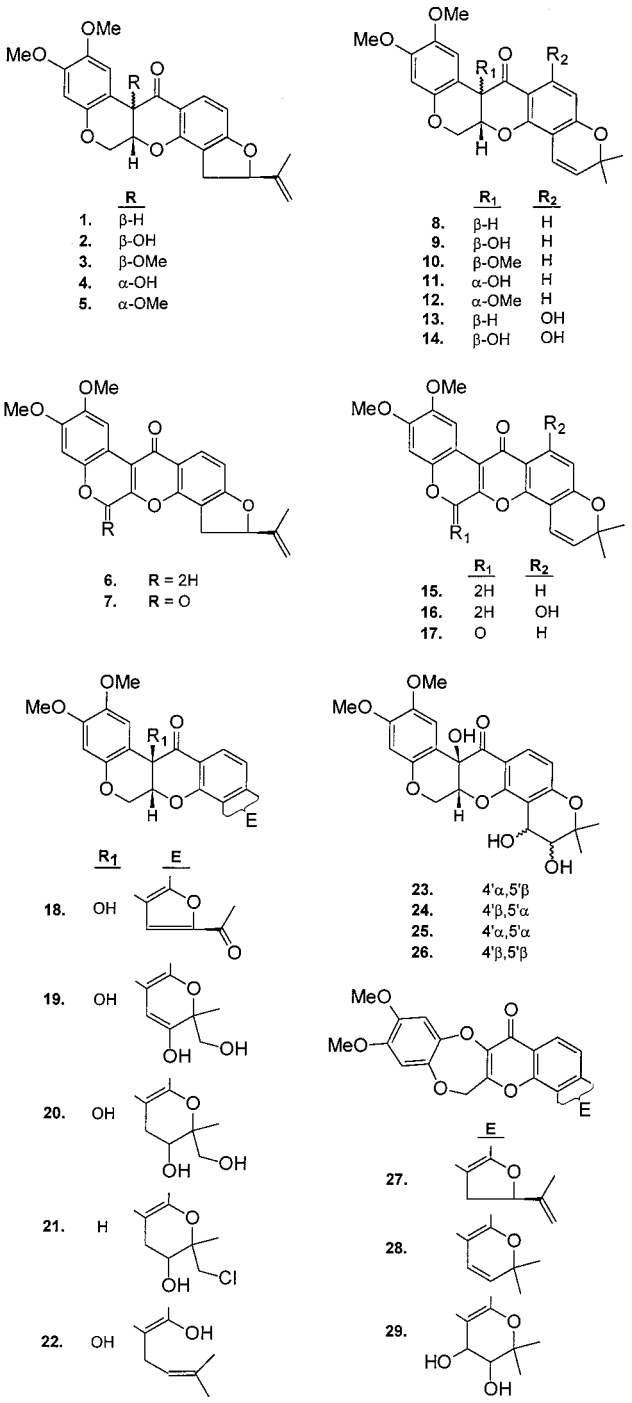

Figure 2. Twenty-nine rotenoids in cubé resin insecticide.

MATERIALS AND METHODS

Caution: *Rotenoids include compounds of high toxicity and should therefore be used under containment conditions.*

Cubé Resin Extraction and Chromatography. The cubé resin studied, designated the original "brittle", was a commercial sample (provided by AgrEvo Environmental Health, Montvale, NJ) in the form used directly as a pesticide. It was from the roots of *L. utilis* and *urucu* collected in the Apurimac River Valley of Peru. They were extracted with trichloroethylene, and the extract was processed by the SARPAP Co. of Bergerac in France. For fractionation, cubé resin was dissolved in warm MeOH (60 °C) by stirring, and major component **1** precipitated at 0 °C. The soluble portion, following filtration and solvent evaporation under reduced pressure, was fractionated on a silica gel column (200−425 mesh) packed in 95% solvent A (hexane) with 5% solvent B (EtOAc/MeOH, 3:1) and developed initially with the same solvent and then a gradient gradually increasing to pure solvent B. Twenty fractions were collected (Fang and Casida, 1997) with the rotenoids appearing in fractions 4−16. Further purification of the rotenoid fractions was achieved by precoated silica gel GF plates (2 mm, 20 × 20 cm) using toluene/acetone (7:3) and/or HPLC performed on a 5-μm C18 column (25 cm × 10 mm i.d.) eluted with gradients of MeCN in H_2O from 20 to 50% in 40 min at a flow rate of 4 mL/min, monitoring the eluent at 310 nm. Four major rotenoids (77%) were obtained (Fang and Casida, 1998) plus 25 minor rotenoids (<0.5% each) considered here. The other components included 11 minor identified flavonoids and stilbenes (Fang and Casida, 1999) and compounds not detected by UV absorbance at 310 nm.

Spectroscopy. ^{1}H and ^{13}C NMR spectra were determined for $CDCl_3$ solutions (unless otherwise stated), reporting chemical shifts (δ in parts per million) relative to the internal standards tetramethylsilane and $CDCl_3$, respectively. ^{13}C NMR resonances are assigned from fully coupled spectra. Electron impact (EI)-MS was accomplished at 70 eV and 200 °C source temperature. Fast atom bombardment (FAB)-MS (both low and high resolutions) was conducted with the Fisons ZAB2-EQ spectrometer. Optical rotation determinations were made with a Perkin-Elmer 241 polarimeter.

X-ray Crystallography. Data were collected using a Syntex $P2_1$ diffractometer equipped with a locally modified LT-1 low-temperature apparatus, a cold stream of 130 K, and an ω scan of 2.2° with a 1.5° offset from the center for left and right background measurements to a maximum 2θ of 130° (graphite monochromated Cu Kα radiation). The structure was solved by direct methods in the space group $P2_1/c$ and refined by full-matrix least-squares (based on F^2) (Sheldrick, 1997). Except for the hydroxyl groups, hydrogen atoms were added geometrically and refined using a riding model and isotropic U's tied to those of the bonded atoms. Two of the hydroxyl hydrogen atoms were located in a difference Fourier map and refined with only a weak restraint that O−H equals 0.84 (2) Å. The third hydroxyl hydrogen (H5′) was assigned a position based upon an algorithm that generates a potential position and adjusts it during refinement to form the best hydrogen bond to an oxygen atom in the structure. Once it was located, it was no longer refined but included in the structure factor calculation. In the final cycles of refinement all non-hydrogen atoms were refined with anisotropic thermal parameters. The inability to obtain a lower R value probably stems from the poor crystal quality of the datum crystal. However, the refinement was unremarkable, and the residual density in the final difference map was <0.37 e Å^{-3}.

Bioassay. Three bioassays were used for the rotenoids under conditions identical to those employed for a series of flavonoids and stilbenes (Fang and Casida, 1999) so that direct potency comparisons can be made for these cubé resin constituents (Fang and Casida, 1998). Inhibition of NADH: ubiquinone oxidoreductase activity was determined with bovine heart electron transport particles as loss of NADH absorbance (Wood et al., 1996; Fang and Casida, 1998). The enzyme (40 μg of protein) and inhibitor (1, 3, 10, 30, etc. nM series) were incubated together for 5 min at 25 °C before addition of NADH to determine residual activity. MCF-7 cells were used to determine the potency of the rotenoids for inhibiting induced ODC activity assayed as $^{14}CO_2$ liberation from L-[1-^{14}C]ornithine (Gerhäuser et al., 1995; Rowlands and Casida, 1997, 1998; Fang and Casida, 1998). The cells in 24-well tissue culture plates were treated with the test compound (concentrations as above) immediately followed by phorbol 12-myristate 13-acetate (200 nM) and then 6 h of incubation before recovery and washing of the cells. The concentration for 50% inhibition (IC_{50}) values (three experiments) were based on the induced portion of the ODC activity, which was generally 3−4-fold relative to the constitutive activity without phorbol ester. Cytotoxicity was evaluated with MCF-7 and Hepa 1clc7 cells using 72 h of exposure to the test compound. Viability was determined with the 3-(4,5-dimethylthiazol-2-yl)-2,5-diphenyltetrazolium bromide colorimetric assay (Fang et al., 1997) using eight replicates to establish IC_{50} values.

STRUCTURAL ASSIGNMENTS OF NEW ROTENOIDS

Isolation and Identification. Chromatographic separation of cubé resin afforded 17 known rotenoids (**1**−**10**, **13**−**16**, **22**, **27**, and **28**) and 12 new ones (**11**, **12**, **17**−**21**, **23**−**26**, and **29**). The known rotenoids were identified by ^{1}H NMR and EI-MS versus authentic standards or by comparison of the spectral data with the corresponding literature values for compounds described earlier. Complete ^{1}H and ^{13}C NMR data for **4** and **5** are presented here for the first time and used in the identification of related compounds (see Supporting Information). Cubé resin constituents of particular interest are the first chlororotenoid in a plant extract (**21**) and four chromatographically separated and stereochemically assigned isomers (**23**−**26**) of a dihydrodiol derivative of tephrosin (**9**). The basis for the structural assignment of each new rotenoid is given below.

Compound 11 is identified by comparison of its ^{1}H and ^{13}C NMR spectra with the corresponding data for **4** (12aα-hydroxyrotenone) and **9** (12a*β*-hydroxydeguelin) (Luyengi et al., 1994). On this basis, **11** has the same A−D-ring system as **4** and the same E ring as **9**. The downfield shift of H-1 (*δ* 7.84) in trans-isomer **11**, compared with that (*δ* 6.56) for cis-isomer **9** results from the negative 12-carbonyl long-range shielding due to the rigid and fairly flat trans-B/C fusion (Begley et al., 1993). The EI mass spectrum exhibits a molecular ion at *m*/*z* 410 (15%) in accord with a formula of $C_{23}H_{22}O_7$. Therefore, the structure of **11** is 12aα-hydroxydeguelin.

Compound 12, in its EI mass spectrum, has a molecular ion at *m*/*z* 424 (85%) in accord with a $C_{24}H_{24}O_7$ formula and base peak at *m*/*z* 222 resulting from cleavage of the intact A- and B-ring fragment (Kostova and Mollova, 1994), suggesting identical A and B rings for **12** and **5** (12aα-methoxyrotenone). The 12a-methoxyl group of **12** is confirmed by a ^{1}H NMR signal (3H, s) at *δ* 3.24 (Crombie and Lown, 1962). Compounds **11** and **12** have the same 12aα configuration and dimethylpyran for the E ring based on ^{1}H and ^{13}C NMR. Therefore, the structure of **12** is 12aα-methoxydeguelin.

Compound 17 gives a ^{1}H NMR signal for H-1 in a characteristic low field (*δ* 9.01), with other signals for protons in the rotenoid A−D-ring system indicating that **17** and known compound **7** (Carlson et al., 1973) have the same 6-oxo-6a,12a-dehydro A−D-ring structure. The ^{1}H NMR signals for the E ring, compared to the corresponding signals of **8**, suggest that **17** is the dimethylpyran analogue of **7**. Finally, the full set of EI-MS data are essentially identical for **17** and **7** (as for **12** versus **5** above and **8** versus **1** in the deguelin and rotenone series, respectively), and the unusually high melting points [mp 282−286 °C for **17** and 298−301 °C for **7** (Begley et al., 1993)] support the structure 6-oxo-6a,12a-dehydrodeguelin for **17**.

Compound 18 ^{1}H and fully coupled ^{13}C NMR spectral data are similar to those of **2** (unpublished results) except for the E ring. The presence of a double bond at C-4′ and 5′ of **18** is evident from the two ^{13}C NMR signals at *δ* 107.5 (d) for C-4′ and 160.7 (s) for C-5′ and the absence of a ^{1}H NMR signal for H-5′. The 5′-substituent is no longer isopropenyl, but instead there is a carbonyl group (*δ* 187.4, s) and a modified methyl group. The downfield shift of the ^{1}H NMR signal of 8′-Me from *δ* 1.79 for **2** to 2.57 for **18** supports the carbonyl group at C-6′ of **18**. This conclusion was confirmed by HR-FABMS ($C_{22}H_{18}O_8$). Compound **18** is, therefore, 7′-nor-6′-oxo-4′,5′-dehydrorotenolone.

Table 1. ^{1}H (300 MHz) and ^{13}C NMR (75 MHz) Data (*δ*) in $CDCl_3$ for 21

position	^{1}H		^{13}C	
	21-I[a]	**21-II**[a]	**21-I**[a]	**21-II**[a]
1	6.75 s (2H)		110.76 d	
1a			104.83 s	
2			144.06 s	
3			149.73 s	
4	6.45 s (2H)		101.14 d	
4a			147.54 s	
6	4.62 dd (*J* = 12.3, 3.1 Hz, 2H, 6 eq) 4.19 d (*J* = 12.3 Hz, 2H, 6 ax)		66.28 t	
6a	4.93 m (2H)		72.36 d	
7a			157.93 s	
8			113.21 s	113.30 s
9			166.71 s	166.83 s
10	6.47 d (*J* = 8.7 Hz, 1H)	6.49 d (*J* = 8.7 Hz, 1H)	104.83 d	
11	7.83 d (*J* = 8.7 Hz, 2H)		129.96 d	
11a			113.69 s	113.75 s
12			188.93 s	
12a	3.85 d (*J* = 3.6, Hz, 2H)		44.71 d	
4′	3.19 d (*J* = 8.7 Hz, 1H)	3.21 d (*J* = 8.7 Hz, 1H)	26.98 t	27.07 t
5′	4.93 m (2H)		86.76 d	87.42 d
6′			72.96 s	73.59 s
7′	3.60−3.76 m (4H)		50.07 t	51.18 t
8′	1.30 s (3H)	1.32 s (3H)	20.03 q	20.66 q
2-OMe	3.81 s (6H)		56.45 q	
3-OMe	3.76 s (6H)		55.88 q	

[a] The designations I and II refer to two proposed isomers with different stereochemistries of the E ring.

Compound 19 has the formula $C_{23}H_{22}O_9$ (HR-FABMS), which means that it has two more oxygens than **9** (Luyengi et al., 1994). The ^{1}H and fully coupled ^{13}C NMR spectra suggest that **19** is an analogue of **9** differing only in a dihydroxylated E ring. The ^{1}H NMR signals of H-5′ (1H) of **9** disappear and a doublet for H-4′ of **9** is converted to a singlet in the spectrum of **19**, indicating 5′-hydroxylation for **19**. The singlet at *δ* 1.37 (7′-Me) for **9** (Luyengi et al., 1994) is replaced by two proton signals at *δ* 3.94 (br d) and 3.64 (br d), which collapse to sharp doublets after addition of D_2O to the $CDCl_3$, providing evidence for 7′-hydroxylation for **19**. Thus, we assign **19** as 5′,7′-dihydroxytephrosin.

Compound 20 by HR-FABMS gives a formula of $C_{23}H_{22}O_9$, which is two more hydrogens than that of **19**. The ^{1}H and ^{13}C NMR spectral data for **20** suggest it is related to **19** with reduction of the double bond in the E ring. Instead of two signals at *δ* 160.2 (s, C-5′) and 100.8 (d, C-4′) as in **19**, a doublet and a triplet appear at *δ* 87.3 (C-5′) and 26.7 (C-4′), respectively, for **20**. Reduction of the double bond between C-4′ and 5′ is supported by three ^{1}H NMR signals for H-4′ (2H) and H-5′ (1H) of **20**. Thus, the structure of compound **20** is 4′,5′-dihydro-5′,7′-dihydroxytephrosin as a single enantiomer of undefined stereochemistry.

Compound 21 contains one chlorine based on an HR-FABMS of $C_{23}H_{23}O_7Cl$ with appropriate $^{35}Cl/^{37}Cl$ ratio. An important diagnostic fragment at *m*/*z* 192 (32%) derived by retro-Diels−Alder processes indicates the same A−D rings as in **8** (Kostova et al., 1988), and the possible difference between **21** and **20** is that one hydroxyl group in the E ring of **20** is replaced by chlorine in the structure of **21**. The ^{1}H and ^{13}C NMR signals of the A−D-ring system (1, 4, 6, 6a, 10, 11, and 12a) support an identical structure in this region for **21** (Table 1) and **8** (Fang and Casida, 1997). Replacing one hydroxyl group of **20** with chlorine as in **21** does not result in a significant difference between the ^{1}H NMR signals for protons in the E ring. However, the chloro

substituent is assigned to C-7′ from the ^{13}C NMR spectral data: the signal at δ 66.8 (t) for C-7′ of **20** undergoes a high-field shift to δ 50.1 for C-7′ of **21**, whereas the signal for C-5′ shows no difference. Therefore, compound **21** is 7′-chloro-5′-hydroxy-4′,5′-dihydrodeguelin. The ^1H and ^{13}C NMR data (Table 1) indicate that **21** may be a mixture of two isomers which have different stereochemistries of the E ring but appear as a single peak in silica gel or C18 HPLC.

Compound 22 is identified as 12aβ-hydroxyrot-2′-enonic acid, previously isolated from the roots of *Millettia pachycarpa* (Singhal et al., 1982). The reported MS and ^1H NMR data (60 MHz, $CDCl_3$) are similar to those of **22** (300 MHz, $CDCl_3$) except the signal for H-6a: δ 4.90 in Crombie and Lown (1962) and δ 4.57 for **22**. We present in the Supporting Information the data of HR-FABMS, ^1H NMR, and ^{13}C NMR not reported before.

Compound 23 has the same skeleton as tephrosin (**9**) (Luyengi et al., 1994) with differences at C-4′ and -5′. The two doublets (J = 9.8 Hz) at δ 6.64 (H-4′) and 5.55 (H-5′) observed for **9** are replaced by signals at δ 4.77 (br d, J = 7.2 Hz, H-4′) and 3.72 (dd, J = 7.2 and 3.6 Hz, H-5′) for **23**. The signals for H-4′ and -5′ of **23**, on addition of D_2O, collapse to sharp doublets with disappearance of signals at δ 3.49 (br s) and 2.88 (d, J = 3.6 Hz), indicating 4′,5′-dihydroxyl groups. The ^{13}C NMR signals for C-4′ and 5′ at δ 67.1 and 74.7 confirm this conclusion. The same cis B/C ring fusion and absolute 6aβ,12aβ (6a*R*,12a*R*) configuration as in **9** are strongly supported by comparison of ^1H and ^{13}C NMR spectra between **23** and **9**. Therefore, compound **23** is the 4′,5′-dihydroxyl derivative of **9**. The MS result is consistent with the interpretation of the ^1H and ^{13}C NMR. Compound **23** exhibits an EI molecular ion peak at *m*/*z* 444 (100%) in accord with $C_{23}H_{24}O_9$, which is two more hydroxyl groups than in **9**. Also, the prominent peaks at *m*/*z* 208 (88%) and 207 (24%) involve cleavage of the intact A- and B-ring fragment and confirm the identical A−D-ring system between **9** (Luyengi et al., 1994) and **23**. Thus, we assigned **23** as 4′,5′-dihydro-4′,5′-dihydroxytephrosin.

The stereochemistry of **23** is assigned by X-ray crystallography. It crystallizes as extremely small needles and plates with considerable twinning. A small plate was selected that gave good diffraction, although peak widths at the base were ~2° in ω. An ORTEP drawing of **23** provides the relative configuration of all ring substituents and the atom labeling scheme (Figure 3). Atoms H6A, O12A, and O5′ occupy the same side of the ring and are labeled β-substituents, the same as known for O12A of **9**. O4′ occupies the opposite side of the ring and is therefore designated an α-substituent. Compound **23** with the 6a*R*,12a*R* configuration of **9** is therefore assigned as (6a*R*,12a*R*,4′*R*,5′*S*)-4′,5′-dihydro-4′,5′-dihydroxytephrosin (Figure 3).

Compounds 23−26 are isomers with different 4′,5′-configurations; they have almost the same mass spectra, and their ^1H and ^{13}C NMR data are nearly identical except for slight differences in ^1H and ^{13}C signals at positions 4′ and 5′ (Table 2). Separation of the four isomers was achieved by TLC and/or HPLC. Compounds **23** and **25** are obtained as needle crystals and **24** and **26** as white solids. Using the *cis*- and *trans*-3,4-diol derivatives of precocene I as model compounds (Halpin et al., 1982; Jennings, 1982; Boyd et al., 1996), the more polar isomers (**23** and **24**) with lower R_f values in silica gel TLC and shorter t_R values in C18 HPLC and larger coupling constant of $J_{4',5'}$ are assigned the trans 4′,5′-configuration, and the less polar isomers (**25** and **26**) with smaller coupling constant of $J_{4',5'}$ are the cis-isomers. Signals for H-4′ of the cis-isomers (**25** and **26**) appear at δ 4.98, and those for the trans-isomers (**23** and **24**) are at higher field (δ 4.77). Also, the chemical shifts for carbons at positions 4′ and 5′ are clearly affected by the 4′ and 5′ stereochemistry. The optical rotations, compared with those for the *cis*- and *trans*-3,4-diol derivatives of precocene I, allow the final stereochemical assignments of **23**−**26**. The 4′*R* and 4′*S* enantiomers have positive and negative optical rotations, respectively, in both precocene I diols (trans and cis) (Halpin et al., 1982; Jennings, 1982; Boyd et al., 1996). Rotenoids **23** (trans) and **25** (cis) with positive optical rotation contributed by the 4′,5′-diol (Table 2) should have the 4′*R* configuration, which is consistent with the X-ray analysis. Correspondingly, isomers **24** and **26**, with large negative optical rotations relative to **8**, should have the 4′*S* configuration. Thus, we designate **24** as (6a*R*,12a*R*,4′*S*,5′*R*)-4′,5′-dihydro-4′,5′-dihydroxytephrosin, **25** as (6a*R*,12a*R*,4′*R*,5′*R*)-4′,5′-dihydro-4′,5′-dihydroxytephrosin, and **26** as (6a*R*,12a*R*,4′*S*,5′*S*)-4′,5′-dihydro-4′,5′-dihydroxytephrosin.

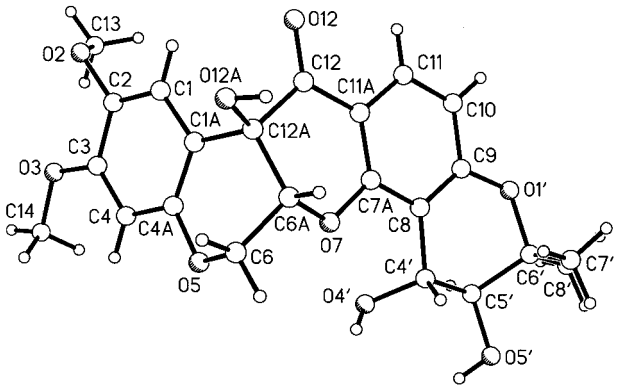

Figure 3. Computer-generated perspective drawing of (6a*R*,12a*R*,4′*R*,5′*S*)-4′,5′-dihydro-4′,5′-dihydroxytephrosin (**23**) based on X-ray crystal analysis. The structure is centrosymmetric, and the inverted epi configuration 6a*S*,12a*S*,4′*S*,5′*R* was also observed. Although epimerization occurs here on modification at the 6a and 12a positions, all rotenoids are arbitrarily shown with retention of the 6a*R* configuration. Crystallographic data for the structure of **23** are available as deposition number 101661 at the Cambridge Crystallographic Data Centre. Copies of the data can be obtained free of charge from CCDC, 12 Union Road, Cambridge CB2 1EZ, U.K.; fax (+44) 1223-336-033; e-mail deposit@chemcrys.cam.ac.uk.

Compounds 27−29 vary only in the E ring. The reference compound in this series is **27**, assigned by X-ray structure determination, with **28** then identified by spectroscopy in comparison with **27** (Fang and Casida, 1997). The structure of **29** is deduced from its ^1H and ^{13}C NMR data compared with those for **23** and **28**. The comparisons indicate that **29** and **28** have the same A−D-ring system and **29** and **23** have the same E ring, a conclusion consistent with the formula $C_{23}H_{22}O_9$ suggested by HR-FABMS. Thus, the structure of **29** (which is enantiomerically pure) is 4′,5′-dihydro-4′,5′-dihydroxy-13-*homo*-13-oxa-6a,12a-dehydrodeguelin; the stereochemistry at 4′ and 5′ is not assigned.

Origin of Newly Described Rotenoids in Cubé Resin. The four major components (**1**, **2**, **8**, and **9**) originate from biosynthesis. Most of the other rotenoids may be decomposition products from crushing the roots

Table 2. Selected Properties of 4′,5′-Dihydro-4′,5′-dihydroxytephrosin Isomers (23−26)

	4′*R*,5′*S* (**23**)	4′*S*,5′*R* (**24**)	4′*R*,5′*R* (**25**)	4′*S*,5′*S* (**26**)
optical rotation, $[\alpha]^{25}_D$ ($CDCl_3$, *c* 1)	−56.5 (+35.0)[a]	−124.0 (−32.5)	−63.4 (+28.0)	−101.2 (−9.7)
^{13}C NMR (δ, $CDCl_3$)				
C-4′	67.1	67.1 d	61.7	62.1 d
C-5′	74.7	74.8 d	70.6	70.6 d
C-6′	79.6	79.6 s	79.1	79.0 s
7′-Me	25.5	25.7 q	24.7	24.7 q
8′-Me	19.9	20.0 q	22.1	22.4 q
^1H NMR (δ, $CDCl_3$)[b]				
H-4′	4.77 br d (*J* = 7.2 Hz)	4.77 br d (*J* = 6.7 Hz)	4.98 br d (*J* = 5.1 Hz)	4.98 br d (*J* = 4.6 Hz)
H-5′	3.72 dd (*J* = 7.2, 3.6 Hz)	3.72 br d (*J* = 6.7 Hz)	3.77 dd (*J* = 5.1, 4.6 Hz)	3.75 br d (*J* = 4.6 Hz)
Me-7′	1.46 s	1.47 s	1.41 s	1.45 s
Me-8′	1.27 s	1.20 s	1.39 s	1.29 s
4′-OH	3.49 br s	3.71 br s	3.62 br s	3.64 br s
5′-OH	2.88 d (*J* = 3.6 Hz)	3.09 br s	3.10 d (*J* = 4.6 Hz)	3.11 br s
C18−HPLC (t_R = min)[c]	13.0	12.0	17.8	16.2
TLC (R_f)[d]				
T:A	0.31	0.28	0.44	0.36
H:E	0.37	0.39	0.43	0.48

[a] Values in parentheses are relative to tephrosin (**8**) $[\alpha]^{25}_D$ −91.5 ($CDCl_3$, *c* 1). [b] On addition of D_2O, the OH signals disappear and the H-4′ and 5′ signals collapse to sharp doublets. [c] 25% MeCN in water. [d] TLC solvent: T:A, toluene/acetone (7:3); H:E, EtOAc/hexane (3:2).

(i.e., initiated by hydrogen peroxide), extracting with trichloroethylene, heating for solvent evaporation, and storing the resin (e.g., the influence of metal traces such as iron from containers). All of these factors point to free radical processes, and the origin of individual products, although speculative, is considered below.

New compounds **11**, **12**, and **17** in the deguelin series were previously known by type as decomposition products in the rotenone series (**4**, **5**, and **7**, respectively) (Crombie, 1963). Rotenone derivative **18** possibly originates from oxidative aromatization of the E ring and then an oxidation, hydrolysis, and oxidative carbon−carbon bond cleavage sequence.

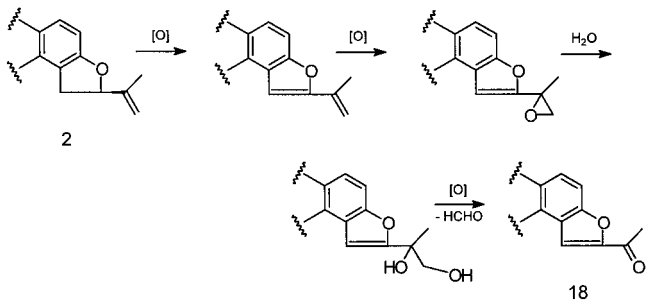

The dimethylchromene of **19**−**21** is modified at a methyl substituent by introduction of chloro or hydroxyl and at the ring by adding a hydroxyl moiety with or without reduction. Equilibration of a dimethylchromene (**a**) with a dienone structure (**b**) is well established (Becker and Michl, 1966; Turchi et al., 1993) under conditions of moderate heat and light, and structure **b** is well set up to stabilize a radical initiated by valence change in a metal impurity introduced during extraction or storage. Radical **c** can react with oxygen to give peroxyl radical **d** (which initiates a chain reaction) followed by hydrolysis to the alcohol (**e**) and hydrogen peroxide. Alternatively, radical **c** will abstract halogen from a chlorinated solvent (e.g., trichloroethylene) to give **f**. The substituted dienone can then recyclize, the equilibrium being well to the chromene side.

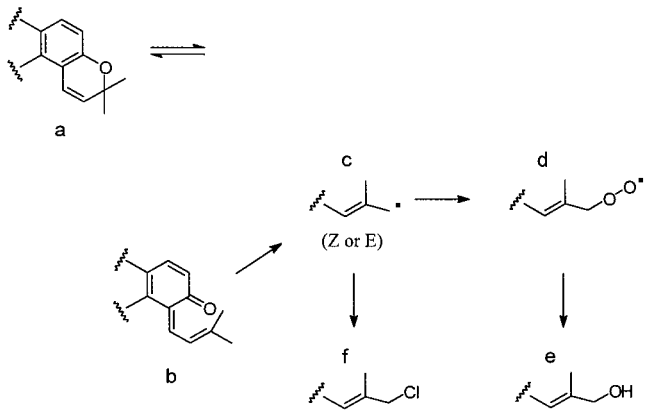

The hydroxyl functionality in the E ring of **19**−**21** is always in the 5′ position, possibly involving the 4′,5′-epoxide intermediate by a multistep undefined reaction sequence. Compounds **23**−**26** probably originate from chemical epoxidation at both the α- and *β*-faces and hydrolysis involving hydroxyl insertion at either of the two flanks to give the four diols. The 13-*homo*-13-oxa-6a,12a-dehydrorotenoids (**27**−**29**) may be formed on extraction and workup because **27** and **28** are found in about equal amounts (Fang and Casida, 1997) and could originate from **1** and **8**, respectively, which are in a 2:1 ratio (Fang and Casida, 1998). These are all minor products but of interest as components in the commercial insecticide/pesticide, at least under the extraction and workup conditions used. Some of these compounds are probably present in most cubé resin insecticidal preparations, whereas others would be dependent on the specific extraction and storage methods that determine the extent of free radical processes and the possibility with chlorinated solvents of chlororotenoid formation.

STRUCTURE−ACTIVITY RELATIONSHIPS

Effect of Structure on Activity in Three Systems. The 29 rotenoids are compared for potency as inhibitors of NADH:ubiquinone oxidoreductase and phorbol ester-induced ODC activities and cell growth in Table 3. In general, similar structure−activity relationships were observed in the three assays, indicating that inhibition of NADH:ubiquinone oxidoreductase activity may be the initial step leading to both inhibition of induced ODC activity and cytotoxicity (Gerhäuser et al., 1996; Rowlands and Casida, 1997, 1998; Fang and Casida, 1998). More specifically for both enzyme as-

Table 3. Biological Activities of Cubé Resin Rotenoids

compound	enzyme activity (IC_{50}, nM)[a] NADH:ubiquinone oxidoreductase	enzyme activity (IC_{50}, nM)[a] phorbol ester-induced ornithine decarboxylase	cell growth (IC_{50}, nM) MCF-7	cell growth (IC_{50}, nM) Hepa 1clc7
rotenone and its derivatives				
1	4.4 ± 1.4	0.8 ± 0.1	450	240
2	290 ± 80	91 ± 3	870	240
3	16 ± 1	190 ± 7	2050	700
4	2010 ± 180	1630 ± 90	10500	10000
5	3660 ± 300	1600 ± 160	15000	26000
6	8600 ± 25	>10000	14500	>30000
7	>10000	>10000	>30000	>30000
18	1600 ± 190	210 ± 40	>30000	13500
22	9900 ± 30	>10000	>30000	>30000
27	115 ± 16	95 ± 4	5300	7000
deguelin and its derivatives				
8	6.9 ± 0.9	11 ± 1	8000	3400
9	98 ± 7	150 ± 30	>30000	23500
10	21 ± 2	480 ± 40	>30000	>30000
11	>10000	5600 ± 0	>30000	>30000
12	>10000	3700 ± 210	>30000	>30000
13	18 ± 2	810 ± 10	27000	13000
14	300 ± 7	370 ± 30	13800	11500
15	1600 ± 200	3500 ± 180	5700	7500
16	>10000	>10000	>30000	>30000
17	>10000	9900 ± 270	>30000	>30000
19	>10000	>10000	>30000	>30000
20	>10000	>10000	>30000	>30000
21	135 ± 7	420 ± 30	11000	14,200
23	>10000	>10000	>30000	>30000
24	>10000	>10000	>30000	>30000
25	>10000	>10000	>30000	>30000
26	>10000	>10000	>30000	>30000
28	140 ± 40	810 ± 20	23000	5300
29	9900	>10000	20000	21500

[a] Mean ± SE, $n = 3$. Although the specific numbers were not reported before, the data points are given in a correlation plot by Fang and Casida (1998).

says, the rotenone series (**1**−**7**) and deguelin series (**8**−**17**) with modifications in the B, C, and D rings follow similar overall substituent effects on activity. The parent compounds (**1** and **8**) are more potent than any of their derivatives. Some activity is retained in both series with 12aβ-hydroxyl (**2** and **9**), 12aβ-methoxyl (**3** and **10**), or 13-*homo*-13-oxa-6a,12a-dehydro (**27** and **28**) and in the deguelin series with 11-hydroxyl (**13**) or 11,12a-dihydroxyl (**14**). Compounds of very low potency are those with 12aα-hydroxyl (**4** and **11**), 12aα-methoxyl (**5** and **12**), 6a,12a-dehydro (**6** and **15**), or 6-oxo-6a,12-dehydro (**7** and **17**). Thus, hydroxylation or methoxylation in the A−D-ring system, including 11 and/or 12a, considerably reduces enzyme inhibitory potency. The trans isomers (**4**, **5**, **11**, and **12**) are 7−>100-fold less active than the corresponding cis isomers (**2**, **3**, **9**, and **10**, respectively) for the 12a-hydroxy and 12a-methoxy derivatives of rotenone and deguelin, and the planar 6a,12a-dehydrorotenoids (compounds **6**, **7**, and **15**−**17**) are of very low activity, indicating the importance of the dihedral angle between the A and D rings (Fang et al., 1997). Variation in the E ring, although not importantly affecting the overall conformation of the molecule (Fang et al., 1997), has a major effect on enzyme inhibitory activity. Dihydroxylation in the dimethylchromen moiety (compounds **23**−**26**) destroys essentially all bioactivity, and the novel 7′-chloro-5′-hydroxy-4′,5′-dihydrodeguelin (**21**) is of only moderate potency, suggesting that the unmodified E ring of deguelin is important for high activity at the target site. Clearly the ligand-binding site interactions leading to enzyme inhibition are strongly influenced by the overall molecular conformation and E-ring substituents. Cytotoxicity is generally lower in the **8** than the **1** series**,** possibly conferred by cytochrome P450-dependent detoxification (Fang et al., 1997), providing a potential advantage for deguelin as a candidate chemopreventive agent (Gerhäuser et al., 1995, 1997). The same structure−activity relationships are observed with MCF-7 and Hepa 1c1c7 cells. The present study does not compare normal cells with tumor cell lines for selectivity, if any, in enzyme inhibition and cytotoxicity.

Toxicological Significance of Rotenoid Constituents in Cubé Resin. Considering their potency and amount, the four major rotenoids (**1**, **2**, **8**, and **9**) account for >95% and probably almost all of the biological activity of the cubé resin examined as an inhibitor of NADH:ubiquinone oxidoreductase and induced ODC activities (Fang and Casida, 1998). They are also the principal cytotoxicants. The minor rotenoids in cube resin are probably in the most part decomposition products from free radical processes during sample preparation, extraction, and processing of the resin and are not important contributors to the biological activity in the systems examined.

ABBREVIATIONS USED

EI, electron impact; FAB, fast atom bombardment; IC_{50}, concentration for 50% inhibition; ODC, ornithine decarboxylase.

ACKNOWLEDGMENT

We thank our laboratory colleagues J. Craig Rowlands, Yoshihisa Tsukamoto, and Gary Quistad for advice and assistance. Professor Leslie Crombie (The University of Nottingham, Nottingham, U.K.) provided

helpful comments. Crystallographic analyses were made by Marilyn Olmstead of the Department of Chemistry, University of California at Davis.

Supporting Information Available: Spectral characterization data for **4**, **5**, **11**, **12**, **17**−**26**, and **29**. This material is available free of charge via the Internet at http://pubs.acs.org.

LITERATURE CITED

Becker, R. S.; Michl, J. Photochromism of synthetic and naturally occurring 2H-chromenes and 2H-pyrans. *J. Am. Chem. Soc.* **1996**, *88*, 5931−5933.

Begley, M. J.; Crombie, L.; Hadi, Hamid bin A.; Josephs, J. L. Synthesis of *trans*-B/C-rotenoids: X-ray and NMR data for cis- and trans- forms of isorotenone. *Chem. Soc. Perkin Trans. 1* **1993**, 2605−2613.

Boyd, D. R.; Sharma, N. D.; Boyle, R.; Evans, T. A.; Malone, J. F.; McCombe, K. M.; Dalton, H.; Chima, J. Chemical and enzyme-catalysed syntheses of enantiopure epoxide and diol derivatives of chromene, 2,2-dimethylchromene, and 7-methoxy-2,2-dimethylchromene (precocene-1). *J. Chem. Soc., Perkin Trans. 1* **1996**, 1757−1765.

California Department of Fish and Game. *Lake Davis Northern Pike Eradication Project, January 1997, Final Environmental Impact Report*; The Resources Agency: Sacramento, CA, 1997.

Carlson, D. G.; Weisleder, D.; Tallent, W. H. NMR investigations of rotenoids. *Tetrahedron* **1973**, *29*, 2731−2741.

Crombie, L. Chemistry of the natural rotenoids. In *Progress in the Chemistry of Organic Natural Products*; Zechmeister, L., Ed.; Springer-Verlag: Vienna, Austria, 1963; Vol. 21, pp 275−325.

Crombie, L.; Lown, J. W. Proton magnetic studies of rotenone and related compounds. *J. Chem. Soc.*, **1962**, 775−781.

Fang, N.; Casida, J. E. Novel bioactive cubé insecticide constituents: isolation and preparation of 13-*homo*-13-oxa-6a,12a-dehydrorotenoids. *J. Org. Chem.* **1997**, *62*, 350−353.

Fang, N.; Casida, J. E. Anticancer action of cubé insecticide: correlation for rotenoid constituents between inhibition of NADH: ubiquinone oxidoreductase and induced ornithine decarboxylase activities. *Proc. Natl. Acad. Sci. U.S.A.* **1998**, *95*, 3380−3384.

Fang, N.; Casida, J. E. New bioactive flavonoids and stilbenes in cubé resin insecticide. *J. Nat. Prod.* **1999**, *62*, 205−210.

Fang, N.; Rowlands, J. C.; Casida, J. E. Anomalous structure−activity relationships of 13-*homo*-13-oxarotenoids and 13-*homo*-13-oxadehydrorotenoids. *Chem. Res. Toxicol.* **1997**, *10*, 853−858.

Fukami, H.; Nakajima, M. Rotenone and the rotenoids. In *Naturally Occurring Insecticides*; Jacobson, M., Crosby, D. G., Eds.; Dekker: New York, 1971; pp 71−97.

Gerhäuser, C.; Mar, W.; Lee, S. K.; Suh, N.; Luo, Y.; Kosmeder, J.; Luyengi, L.; Fong, H. H. S.; Kinghorn, A. D.; Moriarty, R. M.; Mehta, R. G.; Constantinou, A.; Moon, R. C.; Pezzuto, J. M. Rotenoids mediate potent cancer chemopreventive activity through transcriptional regulation of ornithine decarboxylase. *Nat. Med.* **1995**, *1*, 260−266.

Gerhäuser, C.; Kosmeder, J.; Lee, S. K.; Moriarty, R. M.; Pezzuto, J. M. Mechanistic investigation of rotenoid-mediated chemopreventive activity. *Proc. Am. Assoc. Cancer Res.* **1996**, *37*, 278.

Gerhäuser, C.; Lee, S. K.; Kosmeder, J. W.; Moriarty, R. M.; Hamel, E.; Mehta, R. G.; Moon, R. C.; Pezzuto, J. M. Regulation of ornithine decarboxylase induction by deguelin, a natural product cancer chemopreventive agent. *Cancer Res.* **1997**, *57*, 3429−3435.

Halpin, R. A.; El-Naggar, S. F.; McCombe, K. M.; Vyas, K. P.; Boyd, D. R.; Jerina, D. M. Resolution and assignment of absolute configuration to the (+)- and (−)-*cis*- and *trans*-3,4-diol metabolites of the anti-juvenile hormone precocene I. *Tetrahedron Lett.* **1982**, *23*, 1655−1658.

Hollingworth, R. M.; Ahammadsahib, K. I. Inhibitors of respiratory Complex I: mechanisms, pesticidal actions and toxicology. *Rev. Pestic. Toxicol.* **1995**, *3*, 277−302.

Jennings, R. C. Synthesis, resolution and absolute configuration of the diol metabolites of precocene I. *Tetrahedron Lett.* **1982**, *23*, 2693−2696.

Kostova, I. N.; Mollova, N. N. Stereochemical effects in the mass spectra of rotenoids.In *Applications of Mass Spectrometry to Organic Stereochemistry*; Splitter, J. S., Tureček, F., Eds.; VCH: New York, 1994; pp 649−656.

Kostova, I.; Mollova, N.; Ognyanov, I. A mass spectral investigation of rotenoid derivatives. *Izv. Khim.* **1988**, *21*, 236−245.

Luyengi, L.; Lee, I.-S.; Mar, W.; Fong, H. H. S.; Pezzuto, J. M.; Kinghorn, A. D. Rotenoids and chalcones from *Mundulea sericea* that inhibit phorbol ester-induced ornithine decarboxylase activity. *Phytochemistry* **1994**, *36*, 1523−1526.

Negherbon, W. O. *Handbook of Toxicology. Vol. III: Insecticides*; W. B. Saunders: Philadelphia, PA, 1959; pp 661−673.

Rowlands, J. C.; Casida, J. E. Rotenoids inhibit signal transduction pathways which regulate ornithine decarboxylase activity in MCF-7 human breast cancer cells. *Toxicologist* **1997**, *36*, 235.

Rowlands, J. C.; Casida, J. E. NADH: ubiquinone oxidoreductase inhibitors block induction of ornithine decarboxylase activity in MCF-7 human breast cancer cells. *Pharmacol. Toxicol.* **1998**, *83*, 214−219.

Sheldrick, G. M. *SHELXL97. Program for the Solution and Refinement of Crystal Structures*; University of Göttingen: Göttingen, Germany, 1997.

Singhal, A. K.; Sharma, R. P.; Baruah, J. N.; Govindan, S. V.; Herz, W. Rotenoids from roots of *Millettia pachycarpa*. *Phytochemistry* **1982**, *21*, 949−951.

Tomlin, C. D. S., Ed. Rotenone. In *The Pesticide Manual*, 11th ed.; British Crop Protection Council: Farnham, Surrey, U.K., 1997; pp 1097−1099.

Turchi, I. J.; Press: J. B.; McNally, J. J.; Bonner, M. P.; Sorgi, K. L. Interesting contrasts in electrocyclic reactions for thieno[3,2-*b*]-and -[2, 3-*b*]pyrans with chromenes. *J. Org. Chem.* **1993**, *58*, 4629−4633.

Wood, E.; Latli, B.; Casida, J. E. Fenazaquin acaricide specific binding sites in NADH: ubiquinone oxidoreductase and apparently the ATP synthase stalk. *Pestic. Biochem. Physiol.* **1996**, *54*, 135−145.

Received for review November 2, 1998. Revised manuscript received March 4, 1999. Accepted March 5, 1999. The project described was supported by Grant P01 ES00049 from the National Institute of Environmental Health Sciences (NIEHS) of the National Institutes of Health (NIH); its contents are solely the responsibility of the authors and do not necessarily represent the official view of the NIEHS or the NIH.

JF981188X